A Generalized Fokker–Planck Equation Treatment of Inertia and Non-Markovian Effects on the Short-Time Dynamics of a Collision-Induced Reaction

Kazuyasu Ibuki* **and Masakatsu Ueno**

Department of Molecular Science and Technology, Faculty of Engineering, Doshisha University, Tanabe, Kyoto 610-03

(Received August 26, 1996)

The inertia and non-Markovian effects on the short-time dynamics of a diffusion-controlled reaction were studied using a generalized Fokker–Planck equation with a boundary condition suitable for a collision-induced reaction. The approximation of half-range Maxwellian velocity distributions was employed to calculate the time-dependent rate constant. At time zero, the rate constant obtained analytically exhibits a limiting value which is independent of the friction kernels, and is smaller than that of the Smoluchowski–Collins–Kimball (SCK) theory. At finite times, the rate constant is obtained numerically, and its initial decay is slower than that of the SCK theory even when only the inertia effect is taken into account. When a non-Markovian effect is also taken into account, the initial slow decay becomes more pronounced. We have also found that the theoretical rate constant is sensitive to the boundary condition for the velocity distribution at the reaction radius. In order to test the results, we carried out a computer simulation of an encounter reaction between a test particle and hard-sphere reactants in a hard-sphere fluid, and obtained the survival probabilities of the test particle. Our results agree excellently with the simulation results.

The dynamics of diffusion-controlled reactions in solution has been interpreted in terms of the Smoluchowski–Collins–Kimball (SCK) theory[1,2] based on the diffusion equation. Although the SCK theory works well in nanosecond and longer time regimes, an extension is necessary for its applications to subpico- and femtosecond phenomena. In such short-time regions, the effects of the inertia and non-Markovian friction play a key role in determining the molecular migrations, and the simple diffusion equation breaks down due to neglecting the two effects. In a previous paper[3] we proposed an extension of the SCK theory on the basis of Adelman's generalized diffusion equation[4] in which the non-Markovian effect is taken into account. The inertia effect is not treated by Adelman's equation; here, we improve the analysis of the reaction dynamics by taking account of the two effects simultaneously, starting from a generalized Fokker–Planck equation[4,5] (GFPE).

Recently, an extension of the SCK theory was derived by Dong and Andre[6] starting from another type of generalized diffusion equation in which both the inertia and non-Markovian effects were taken into account.[5,7] Their theory clearly indicates the importance of the two effects in the short-time dynamics of a kind of diffusion-controlled reactions. However, this is inapplicable for collision-induced reactions. It is nontrivial to overcome this limitation, because various types of chemical reactions and energy transfer processes are considered to be induced by collisions. The dynamics of molecular collisions are determined not only by the density distribution, but also by the velocity distribution. Hence, a theoretical model for the dynamics of a collision-induced reaction should include a boundary condition for the velocity distribution at the reaction radius in addition to that for the density.[8,9] A large effect of the velocity distribution on the reaction dynamics is expected, particularly at times shorter than the decay of the velocity autocorrelation function. The generalized diffusion equation is concerned only with the density distribution, and cannot be applied for a study of collision-induced reactions. GFPE describes the time evolution of the distribution in phase space; we choose it as a starting equation for investigating the effect of the velocity distribution on the reaction dynamics at short times.

One of the purpose of the present paper is to clarify what type of role is played by the inertia effect, non-Markovian friction, and the boundary condition for the velocity distribution in determining the short-time dynamics of diffusion-controlled reactions. To characterize the dynamic nature of these effects, we have used a simplified model without static potential effects. We approximately solved GFPE with a boundary condition suitable for a collision-induced reaction using the method of half-range Maxwellian distributions originally developed for the ordinary Fokker–Planck equation (OFPE) by Harris.[8,9]

To test the validity of the present results, we carried out a molecular dynamics simulation in a hard-sphere fluid. For the present theory with a simplified model, we think that it is better to compare the results with a simulation than with an experiment; from the latter, we cannot distinguish the shortcomings of the theory from the effects of factors ignored in the theory. We need a system which strictly corresponds to the model employed in the theory for a definite test of

the theory; we can make such a system only by a computer simulation. Once the validity of the theory is confirmed by simulations, we can regard the theory as a reference to elucidate effects of complicated factors which determine the reaction dynamics at short times. For a better understanding of the effects of the distance-dependent reactivity and the potential of mean force, for example, a reference system without these effects is of great importance. Another purpose of the present work is to provide such a reference system.

In the next section we describe the theory and calculate the time-dependent rate constant. The results are compared with other theories in the third section, and tested against a computer simulation in the fourth section.

Theoretical

Model for Reaction. We investigate the dynamics of an encounter reaction between two rigid spheres, A and B. The target molecule A is assumed to be fixed at the origin of the coordinate, and the reactant molecule B migrates in space.

Before the reaction begins, the distribution of B around A is spatially uniform with a Maxwell–Boltzmann velocity distribution,

$$f(\boldsymbol{v},\boldsymbol{r} > R, t \leq 0) = n_0 \left(\frac{m}{2\pi k_B T}\right)^{3/2} \exp\left(-\frac{mv^2}{2k_B T}\right). \quad (1)$$

Here, $f(\boldsymbol{v}, \boldsymbol{r}, t)$ is the distribution function in velocity $\boldsymbol{v}$ and position $\boldsymbol{r}$ at time t, R the reaction radius, n_0 the number density, m the mass of a B molecule, k_B the Boltzmann constant, and T the absolute temperature. The distribution in position (the density) is spherically symmetric because of the symmetry of the problem.

When B collides with A at $r=R$ after $t=0$, they react immediately and B is absorbed by A. This collision-induced reaction of the perfect absorbing case can be expressed by the following boundary condition:[8,9]

$$f(v_r > 0, R, t > 0) = 0, \quad (2)$$

where v_r is the radial component of the velocity given by

$$v_r = \frac{\boldsymbol{v}\cdot\boldsymbol{r}}{r}. \quad (3)$$

Equation 2 means that there are no B molecules rebound from A. It is emphasized by Harris[8,9] that the boundary condition for the perfect absorption is not the so-called absorbing boundary condition, $f(\boldsymbol{v},R,t)=0$. We must be careful concerning the difference. For example, if the density at $r=R$ is zero, the absorption flux, which expresses the reaction rate, becomes zero and the reaction cannot occur.

At an infinite distance, there is another boundary condition that the distribution function remains unchanged. This is expressed by

$$f(\boldsymbol{v}, \infty, t > 0) = n_0 \left(\frac{m}{2\pi k_B T}\right)^{3/2} \exp\left(-\frac{mv^2}{2k_B T}\right). \quad (4)$$

The rate of reaction can be calculated based on the time evolution of the distribution function. The flux $j_r(R, t)$ of B in the direction of the position vector at $r=R$ is given by

$$j_r(R,t) = \int v_r f(\boldsymbol{v},R,t)\,d\boldsymbol{v}, \quad (5)$$

and the time-dependent rate constant $k(t)$ by

$$k(t)n_0 = -4\pi R^2 j_r(R,t). \quad (6)$$

Our model described above can be considered to be ideal fluorescence quenching. When the quenching occurs by an electron transfer, the reactivity usually depends on the distance between the target and the quencher, and the boundary condition (Eq. 2), is not so suitable. When the quenching occurs by an energy transfer, on the other hand, the reaction is considered to be induced by collisions; thus, Eq. 2 is an appropriate choice for the boundary condition. Our model is ideal in the following two aspects: (1) the potential effects are neglected in order to focus attention on the inertia and non-Markovian effects, and (2) the probability of a reaction for a collision is unity. We later extend the boundary condition so as to take into account the effect of a reaction probability that is less than unity.

Generalized Fokker–Planck Equation. In order to incorporate the inertia and non-Markovian effects in the model described above, we assume that the migration of B is governed by the generalized Langevin equation for free motion,

$$\frac{d\boldsymbol{v}(t)}{dt} = -\int_0^t \beta(t-t')\boldsymbol{v}(t')dt' + \frac{\boldsymbol{F}(t)}{m}, \quad (7)$$

where $\beta(t)$ is the time-dependent friction kernel and $\boldsymbol{F}(t)$ the random force. These two quantities satisfy the fluctuation-dissipation relation.[10]

Adelman[4] showed that a generalized Fokker–Planck equation can be derived from Eq. 7 when the random force is a Gaussian random variable. The Gaussian assumption usually provides a good approximation.[11,12] An outline of the derivation is described in Appendix. Adelman's GFPE is given by

$$\frac{\partial f(\boldsymbol{v},\boldsymbol{r},t)}{\partial t} + \boldsymbol{v}\cdot\frac{\partial f(\boldsymbol{v},\boldsymbol{r},t)}{\partial \boldsymbol{r}} = \xi(t)\frac{\partial}{\partial \boldsymbol{v}}\cdot[\boldsymbol{v}f(\boldsymbol{v},\boldsymbol{r},t)] + \xi(t)\frac{k_B T}{m}\frac{\partial^2 f(\boldsymbol{v},\boldsymbol{r},t)}{\partial \boldsymbol{v}^2} + [\gamma(t)-1]\frac{k_B T}{m}\frac{\partial^2 f(\boldsymbol{v},\boldsymbol{r},t)}{\partial \boldsymbol{r}\partial \boldsymbol{v}}. \quad (8)$$

Here, the symbols have the following definitions:[4,5]

$$\gamma(t) = \chi(t) + \xi(t)\psi(t), \quad (9)$$

$$\xi(t) = -\frac{1}{\chi(t)}\frac{d\chi(t)}{dt}, \quad (10)$$

$$\psi(t) = \frac{\langle[\boldsymbol{r}(t)-\boldsymbol{r}(0)]\cdot\boldsymbol{v}(0)\rangle}{\langle v(0)^2\rangle}, \quad (11)$$

$$\chi(t) = \frac{\langle\boldsymbol{v}(t)\cdot\boldsymbol{v}(0)\rangle}{\langle v(0)^2\rangle} = \frac{d\psi(t)}{dt}. \quad (12)$$

The difference between GFPE and OFPE are that the coefficients in GFPE depend on time, and that GFPE has an additional term, i.e., the third term in the right-hand side of Eq. 8. For the Markovian case, for which the time-dependent friction kernel is given by $\beta(t)=2\beta_\infty\delta(t)$, the coefficients in GFPE are independent of time, and given by $\xi(t)=\beta_\infty$ and

$\gamma(t)=1$. Thus, GFPE reduces to OFPE with the friction constant given by β_∞.

For non-Markovian cases, $\xi(t)$ and $\gamma(t)$ largely depend on time. Figure 1 shows the time dependence of $\xi(t)$ and $\gamma(t)$ for a one-component hard-sphere fluid at the reduced density, $\rho^*=0.9428$. The reduced density ρ^* is defined by

$$\rho^* = \rho\sigma^3, \tag{13}$$

where ρ is the number density and σ the diameter of a hard-sphere. The coefficients $\xi(t)$ and $\gamma(t)$ are calculated from the velocity autocorrelation function (vacf) $\chi(t)$ obtained from a molecular dynamics simulation. The details of the simulation will be described later. The reduced variables used in Fig. 1 are defined by

$$\tau = t\beta_\infty \tag{14}$$

and

$$\zeta(t) = \frac{\xi(t)}{\beta_\infty}. \tag{15}$$

The phenomenological friction coefficient β_∞ is calculated by the Einstein relation between the phenomenological diffusion coefficient D_∞ and β_∞, given by

$$D_\infty = \frac{k_BT}{m\beta_\infty} = \frac{k_BT}{m}\int_0^\infty \chi(t)\mathrm{d}t. \tag{16}$$

Since GFPE with time-dependent coefficients is not familiar in chemistry, we briefly explain its important properties. We should first point out that $\xi(0)=0$ and $\gamma(0)=1$ in general, except for hard-core systems, such as the hard-sphere fluid, since $\chi(0)=1$ and $\mathrm{d}\chi(t)/\mathrm{d}t$ is zero at $t=0$. This exhibits a sharp contrast to the previous results[3] based on Adelman's generalized diffusion equation for which the short-time behavior of the time-dependent diffusion constant is quite sensitive to the functional form of $\beta(t)$. Such a behavior of Adelman's generalized diffusion equation is considered to originate from an improper disregard of the inertia effect.[6]

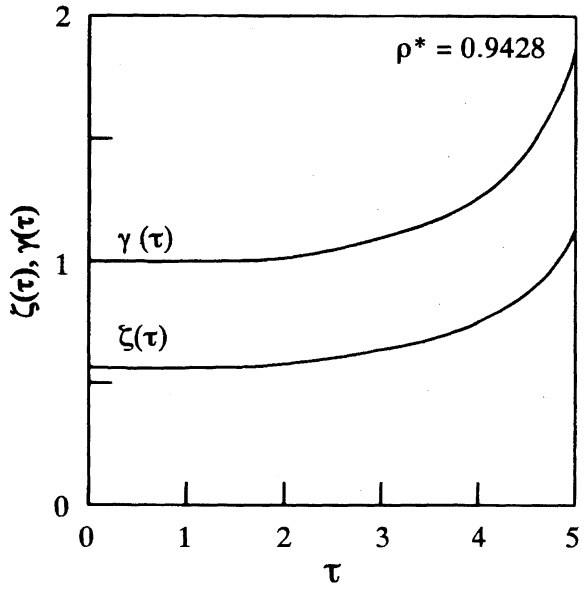

Fig. 1. Time dependence of $\zeta(\tau)$ and $\gamma(\tau)$ for a one-component hard-sphere fluid at $\rho^*=0.9428$.

For a hard-sphere fluid, $\mathrm{d}\chi(t)/\mathrm{d}t$ is not zero at $t=0$,[10] and $\xi(0)$ has a finite value. $\mathrm{d}\chi(t)/\mathrm{d}t$ at $t=0$ is determined by the collision rate. If we assume that the collision rate is given by that of the Enskog theory,[10] $\xi(0)$ is given by the Enskog friction coefficient β_∞^E. At high densities, β_∞ obtained from a molecular dynamics simulation is much larger than β_∞^E,[13,14] and $\xi(0)$ is smaller than β_∞. For $t>0$, the behaviors of $\xi(t)$ and $\gamma(t)$ for a hard-sphere fluid are qualitatively similar to those in general cases.

As can be seen in Eqs. 9 and 10, $\xi(t)$ and $\gamma(t)$ are functions of the inverse of $\chi(t)$. In a dense fluid, since $\chi(t)$ has negative regions, $\xi(t)$ and $\gamma(t)$ diverge when $\chi(t)=0$, and become negative in some time regions. The physical meaning of such behaviors of non-Markovian processes was discussed by Hänggi et al.[15] In a hard-sphere fluid at $\rho^*=0.9428$, $\chi(t)$ becomes zero at about $\tau=5.5$. The steep rises of $\zeta(\tau)$ and $\gamma(\tau)$ in the right-half of Fig. 1 are due to the singularities. San Miguel and Sancho[7] pointed out that, in spite of the singular behavior of its coefficients, time-dependent and stationary solutions exist for GFPE. In this paper we restrict our calculation of the rate constant to time regions before the first singular point for $\xi(t)$ and $\gamma(t)$, since we solve the equations numerically and our main concern is the short-time dynamics of the reaction.

$\xi(t)$ in Eq. 8 corresponds to the friction constant in OFPE. One may feel strange that $\xi(t)$ can become singular and negative. It is obvious from the definition of Eq. 10, however, that $\xi(t)$ is neither the time-dependent friction kernel nor the friction constant itself. The value of $\xi(t)$ is not restricted to be positive and definite. We demonstrate how singular points and negative regions of the coefficients play an important role in GFPE. From Eq. 8 we can derive an equation for the time evolution of vacf $\chi(t)$ by a method similar to the case of OFPE,

$$\frac{\mathrm{d}\chi(t)}{\mathrm{d}t} = -\xi(t)\chi(t). \tag{17}$$

If $\xi(t)$ is always positive and definite, $\chi(t)$ must always be positive and monotonously decreasing, since $\chi(0)=1$ and $\chi(\infty)=0$. This means that vacf with negative regions is not allowed when $\xi(t)$ is positive and definite; OFPE cannot explain vacf with negative regions. Since $\xi(t)$ of GFPE can become singular and negative, $\chi(t)$ with negative regions is allowed in Eq. 17. Moreover, we can easily show that, for the natural boundary, GFPE with singular coefficients reproduces the time evolutions of all the first and second moments of the velocity and position derived from the generalized Langevin equation. This clearly indicates the validity of GFPE.

To clarify the difference between GFPE and OFPE, it is important to note that GFPE does not reduce to OFPE even in the long-time limit, except for the Markovian case. In the long-time limit, the coefficients $\xi(\infty)$ of the first two terms in the right-hand side of Eq. 8 are different from those of OFPE β_∞, and the third terms which is absent in OFPE is non-vanishing since $\gamma(\infty)$ is not unity. The significance of this property of GFPE was discussed in detail by Adelman.[4] The long-time behaviors of $\xi(t)$ and $\gamma(t)$ are closely related

to that of $\chi(t)$. As far as the long-time limiting behavior is concerned, one of the serious limitations of OFPE is that the equation cannot explain the well-known non-exponential tail of vacf in a dense fluid.[13] Adelman clearly showed that, with a proper choice of the time-dependent friction kernel $\beta(t)$, GFPE can reproduce the long-time tail because $\xi(\infty)$ and $\gamma(\infty)$ can be different from the corresponding coefficients in OFPE. The importance of the long-time behavior of $\gamma(t)$ will be discussed again later in relation to the derivation of the steady-state diffusion equation. It should be noted here, however, that GFPE and OFPE have the same equilibrium distribution; the Maxwellian distribution given by Eq. 1 is a solution of Eq. 8 at any time.

Method of Half-Range Maxwellian Velocity Distributions. In order to solve GFPE approximately with the conditions given by Eqs. 1, 2, and 4, we employ the method of half-range Maxwellian velocity distributions developed by Harris.[8] Here, we briefly explain the application of his method to GFPE. In this method, the phase space is divided into two parts: one for $v_r>0$ and another for $v_r<0$. This division is suitable to apply the boundary condition, Eq. 2, to GFPE. The distribution function in each space is approximated by half-range Maxwellian distributions, as follows:

$$f(\boldsymbol{v},r,t)=f_i(\boldsymbol{v},r,t)=2n_i(r,t)\left(\frac{m}{2\pi k_\mathrm{B}T}\right)^{3/2}\exp\left(-\frac{mv^2}{2k_\mathrm{B}T}\right), \quad (18)$$

where $i=1$ for $v_r>0$ and $i=2$ for $v_r<0$. Although the non-equilibrium velocity distribution function is discontinuous at $v=0$ in this approximation, GFPE is reduced to a set of simple equations, which is mathematically more tractable.

With this approximation, the first two moments of v_r are given by

$$n(r,t)=\int f(\boldsymbol{v},r,t)\,\mathrm{d}\boldsymbol{v}=N(r,t), \quad (19)$$

$$j_r(r,t)=\int v_r f(\boldsymbol{v},r,t)\,\mathrm{d}\boldsymbol{v}=\sqrt{\frac{2k_\mathrm{B}T}{\pi m}}M(r,t), \quad (20)$$

where $N(r,t)$ and $M(r,t)$ are defined as

$$N(r,t)=n_1(r,t)+n_2(r,t), \quad (21)$$

$$M(r,t)=n_1(r,t)-n_2(r,t). \quad (22)$$

Substituting Eq. 18 into Eq. 8 and calculating the first two moments of v_r, we obtain the following equations for $N(r,t)$, $M(r,t)$:

$$\frac{\partial N(r,t)}{\partial t}=-\sqrt{\frac{2k_\mathrm{B}T}{\pi m}}\left[\frac{\partial M(r,t)}{\partial r}+\frac{2}{r}M(r,t)\right], \quad (23)$$

$$\frac{\partial M(r,t)}{\partial t}=-\gamma(t)\frac{\pi}{2}\sqrt{\frac{2k_\mathrm{B}T}{\pi m}}\frac{\partial N(r,t)}{\partial r}-\xi(t)M(r,t). \quad (24)$$

Equation 23 is the equation of continuity, and Eq. 24 can be considered as an extension of Fick's law.[8] Eliminating $M(r,t)$ from Eqs. 23 and 24, we can obtain a generalized diffusion equation which is non-local in time,

$$\frac{\partial N(r,t)}{\partial t}=\frac{k_\mathrm{B}T}{m}\mathrm{e}^{-\phi(t)}\int_0^t \mathrm{e}^{\phi(t')}\gamma(t')\left(\frac{\partial^2 N(r,t')}{\partial r^2}+\frac{2}{r}\frac{\partial N(r,t')}{\partial r}\right)\mathrm{d}t', \quad (25)$$

where

$$\phi(t)=\int_0^t \xi(t')\mathrm{d}t'. \quad (26)$$

From the generalized Langevin equation with a Gaussian random force, on the other hand, Mazo[5] rigorously derived a generalized diffusion equation which is local in time (see Appendix). Therefore, Eq. 25, which is non-local in time, clearly indicates the approximate nature of the present method.

We introduce the dimensionless variable defined by Eqs. 14 and 15, and

$$x=r\beta_\infty\sqrt{\frac{\pi m}{2k_\mathrm{B}T}}. \quad (27)$$

For a typical case, such as $D_\infty=1.0\times10^{-9}$ m^2 s^{-1} at room temperature with a molecular weight of 127, the units of τ and x are 1.0×10^{-13} s and 1.1×10^{-11} m, respectively. We thus obtain dimensionless equations as

$$\frac{\partial N(x,\tau)}{\partial\tau}=-\frac{\partial M(x,\tau)}{\partial x}-\frac{2}{x}M(x,\tau), \quad (28)$$

$$\frac{\partial M(x,\tau)}{\partial\tau}=-\gamma(\tau)\frac{\pi}{2}\frac{\partial N(x,\tau)}{\partial x}-\zeta(\tau)M(x,\tau), \quad (29)$$

a dimensionless flux $J_r(x,\tau)$ as

$$J_r(x,\tau)=\frac{j_r(r,t)}{n_0}\sqrt{\frac{\pi m}{2k_\mathrm{B}T}}=\frac{M(x,\tau)}{n_0}, \quad (30)$$

and a dimensionless rate constant $\varkappa(\tau)$ as

$$\varkappa(\tau)=\frac{k(t)}{4\pi R^2}\sqrt{\frac{\pi m}{2k_\mathrm{B}T}}=-J_r(X,\tau), \quad (31)$$

where the dimensionless reaction radius is given by

$$X=R\beta_\infty\sqrt{\frac{\pi m}{2k_\mathrm{B}T}}. \quad (32)$$

Extension of Boundary Condition. Here, we reexamine the boundary condition so as to incorporate the finite reactivity. The initial condition can be expressed by

$$n_1(x,0)=n_2(x,0)=\frac{n_0}{2}, \qquad N(x,0)=n_0, \qquad M(x,0)=0, \quad (33)$$

and the boundary conditions at $\tau>0$ by

$$n_1(\infty,\tau)=n_2(\infty,\tau)=\frac{n_0}{2}, \qquad N(\infty,\tau)=n_0, \qquad M(\infty,\tau)=0, \quad (34)$$

and

$$n_1(X,\tau)=0, \qquad N(X,\tau)=-M(X,\tau). \quad (35)$$

The last equation is our concern here.

As mentioned earlier, Harris' boundary condition, Eq. 35, expresses the situation that the reaction occurs in every collision between A and B. In practice, however, the fraction of the collisions effective for the reaction is always less than unity. We should extend the boundary condition so as to take into account this effect of the finite reactivity. With the help of Eqs. 19 and 20, we can see that Eq. 35 is a kind of the

radiation boundary condition, which is a linear relationship between the density and the flux at the reaction radius. We can extend Harris' condition in the following way:

$$pN(X,\tau) = -M(X,\tau), \tag{36}$$

where p is reactivity parameter; p=1 for the perfect absorption and p=0 for perfect reflection. In the present work, we use the extended boundary condition instead of Eq. 35.

It must be emphasized that the reactivity parameter p is not equivalent to the transmission coefficient α, which is defined as the number of the collisions with reaction divided by the total collision number. The total collision number is proportional not to $N(X,\tau)$, but to $n_2(X,\tau)$, and $n_1(X,\tau)$ is proportional to the number of collisions without a reaction.This results in the following equation:

$$n_1(X,\tau) = (1-\alpha)n_2(X,\tau). \tag{37}$$

Therefore,

$$N(X,\tau) = (2-\alpha)n_2(X,\tau), \qquad M(X,\tau) = -\alpha n_2(X,\tau). \tag{38}$$

Substituting the above equations into Eq. 36, we obtain the following relation between p and α:

$$p = \frac{\alpha}{2-\alpha}, \quad \alpha = \frac{2p}{1+p}. \tag{39}$$

In this paper we use the reactivity parameter p, since we can show a linear relation between p and the intrinsic rate constant k^{int}, which is a parameter which appeared in the SCK theory. The relation will be derived later.

Time Dependence of the Rate Constant. We now calculate the time-dependent rate constant. We use $\zeta(\tau)$ and $\gamma(\tau)$ for a one-component hard-sphere fluid. The reaction radius R is assumed to be the same as the diameter of the hard-sphere σ. We calculate the results at two densities, ρ^*= 0.7856 and 0.9428. At ρ^*=0.7856, vacf can be fitted into a single exponential function within the simulation uncertainty. This means that the non-Markovian effect is negligibly small at this density; we calculate the rate constant using $\zeta(\tau)$ and $\gamma(\tau)$ for the Markovian case in which only the inertia effect is taken into account. At ρ^*=0.9428, we calculate with $\zeta(\tau)$ and $\gamma(\tau)$ shown in Fig. 1; the non-Markovian effect cannot be neglected at this density. Thus, we can discuss the inertia and non-Markovian effects separately by comparing the results at the two densities.

For the Markovian case, Eqs. 28 and 29 can be solved analytically at any time. The Laplace transform of the rate constant is given by

$$\tilde{\varkappa}(s) = \frac{p}{s}\left[1 - \frac{1}{1+\frac{\pi}{2p(s+1)}\left(\sqrt{\frac{2s(s+1)}{\pi}}+\frac{1}{X}\right)}\right]. \tag{40}$$

For p=1, this equation agree with Harris' result.[8,16] The Laplace inversion of Eq. 40 can be carried out numerically.[17]

For the non-Markovian case, we numerically solve Eqs. 28 and 29 subject to the conditions Eqs. 33, 34, and 36 using the Lax–Wendoroff explicit method. The numerical solution is unstable in the first several hundreds steps, but then becomes stable. As is shown later, however, the limiting value at τ=0 can be obtained analytically, and we can interpolate $\varkappa(\tau)$ in the unstable region. Here, on the other hand, we should note the behavior of the solutions for $\tau>0$. Although we calculate $\varkappa(\tau)$ near to the singular point of $\zeta(\tau)$ and $\gamma(\tau)$ for ρ^*=0.9428, there are no signs of divergence in $\varkappa(\tau)$. This fact may support the idea that there exist time-dependent solutions for a GFPE with divergent coefficients.

The time-dependent rate constants thus calculated are shown in Figs. 2 and 3 for ρ^*=0.7856 and 0.9428, respectively. In Fig. 3, the result for the Markovian case is also shown for a comparison. We can recognize the following tendencies from the figures: (1) For the Markovian case, $\varkappa(\tau)$ is a monotonously decreasing function with time. (2) When the non-Markovian effect is present in addition to the inertia effect, the initial decay of $\varkappa(\tau)$ becomes slower. The reason for the slow decays of the rate constants are discussed later in relation to the SCK theory.

Limiting Cases. In the short- and long-time limits, we can analytically calculate the rate constant for the non-Markovian case. We first examine the short-time limit. For the Markovian case, the rate constant given by Eq. 40 has a short-time limiting value,

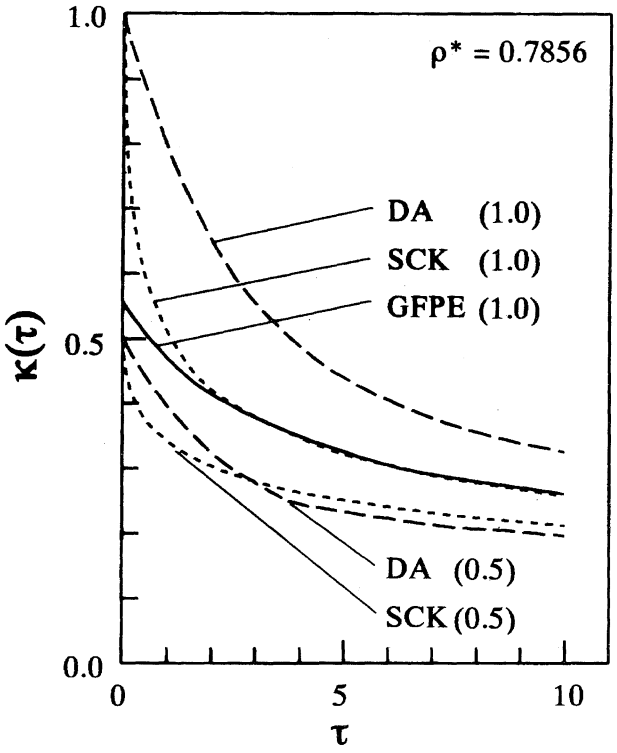

Fig. 2. The time-dependent rate constant in a hard-sphere fluid at ρ^*=0.7856. A solid line indicates the result of the present work. Broken and dotted lines indicate the results of the DA and the SCK theories, respectively. Numbers in the parentheses are the values of the reactivity parameter p.

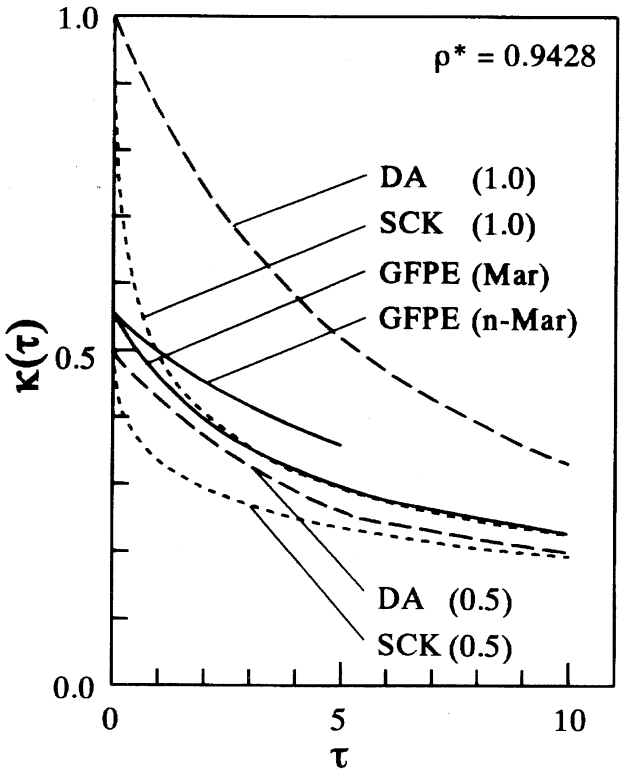

Fig. 3. The time-dependent rate constant in a hard-sphere fluid at $\rho^*=0.9428$. Lines and numbers have the same meanings as in Fig. 2. "Mar" and "n-Mar" indicate the Markovian and non-Markovian cases, respectively. The results of this work are calculated for $p=1.0$.

$$\varkappa(0)=\frac{p\sqrt{\pi/2}}{p+\sqrt{\pi/2}}. \tag{41}$$

For the non-Markovian case with an arbitrary friction kernel, $\gamma(0)=1$ and $\zeta(0)=c$ in Eq. 29, where c is a constant; $c=0$ in general, except for hard-sphere fluids for which $c>0$. Thus, we can obtain the short-time limiting form of Eq. 29 as

$$\frac{\partial M(x,\tau)}{\partial\tau}=-\frac{\pi}{2}\frac{\partial N(x,\tau)}{\partial x}-cM(x,\tau). \tag{42}$$

We can analytically solve Eqs. 28 and 42 for an arbitrary $c\geq 0$ and calculate the short-time limiting value of the dimensionless rate constant by the same method as in the Markovian case. The resultant $\varkappa(0)$ is also given by Eq. 41. We show the reactivity parameter dependence of the initial rate constant in Fig. 4. $\varkappa(0)$ is independent of the time-dependent friction kernel, and increases non-linearly with an increase in p.

We next examine the long-time limit. For the stationary state in the long-time limit, our equations reduce to the steady state diffusion equation. From Eqs. 9, 10, 11, 12, and 15, we can see that $\gamma(\infty)=\zeta(\infty)$. When a stationary state is accomplished in the long time limit, Eq. 29 is written as

$$0=-\frac{\pi}{2}\frac{\partial N}{\partial x}-M, \tag{43}$$

which coincides with the equation derived from OFPE. Substituting Eq. 43 into Eq. 28 and setting the left-hand side of

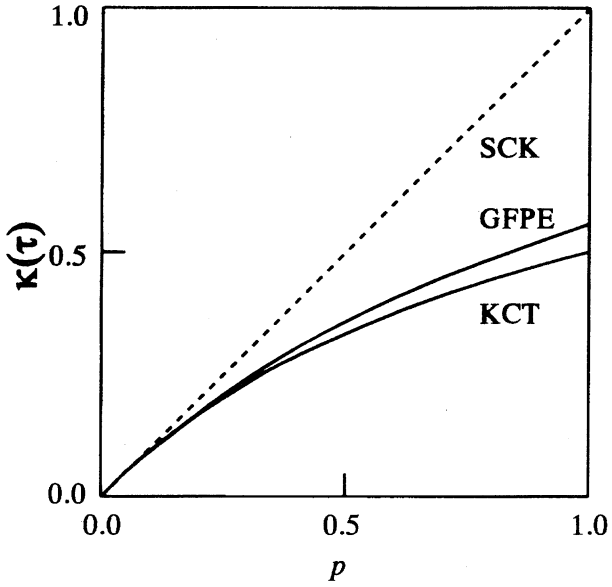

Fig. 4. Reactivity parameter dependence of dimensionless rate constant at $\tau=0$.

Eq. 28 as zero, we obtain

$$0=\frac{\pi}{2}\left(\frac{\partial^2 N(x)}{\partial x^2}-\frac{2}{x}\frac{\partial N(x)}{\partial x}\right). \tag{44}$$

Using the Einstein relation, Eq. 16, for the diffusion coefficient D_∞, Eq. 44 becomes the steady state diffusion equation.

The boundary condition in the long-time limit is obtained by substituting Eq. 43 into Eq. 36,

$$pN(X)=\frac{\pi}{2}\frac{\partial N(x)}{\partial x}\bigg|_{x=X} \tag{45}$$

This equation has the same form as the CK boundary condition,

$$-4\pi R^2 D_\infty\left(\frac{\partial N(r,t)}{\partial r}\right)_{r=R}=k^{\mathrm{int}}N(R,t), \tag{46}$$

where k^{int} is the intrinsic rate constant at the reaction radius. Converting the dimension of Eq. 45 into the ordinary one and comparing it with Eq. 46, we obtain

$$k^{\mathrm{int}}=4\pi R^2 p\sqrt{\frac{2k_{\mathrm{B}}T}{\pi m}}. \tag{47}$$

Therefore, the long-time limiting value of the rate constant of the present treatment coincides with that of the SCK theory with k^{int} given by Eq. 47.

It should be noted that, in spite of the existence of an additional term (the third term in the right-hand side of Eq. 8), which is non-vanishing in the long-time limit, GFPE reduces to the same equation as OFPE.[18,19] If the remaining terms in GFPE were strictly the same as those in OFPE in the long-time limit, this would be unreasonable. As pointed out earlier, however, the long-time limiting value of $\xi(t)$ is different from the phenomenological friction coefficient β_∞. Therefore, we need an additional term to obtain the same equation from GFPE as that from OFPE in the long-time limit. This clearly indicates the importance of the third

term in the right-hand side of Eq. 8. Although we used the approximation, Eq. 18, in the derivation of Eq. 44 from GFPE, we believe that the approximation is not necessary. Mazo[5] derived a generalized diffusion equation, which is reduced to Eq. 44 in the long-time limit from the generalized Langevin equation, Eq. 7, by the same procedure as the derivation of GFPE (see Appendix); we can consider that the long-time limiting form of GFPE can be expressed in the same form as that of the generalized diffusion equation.

Comparisons with Other Theories

Kinetic Collision Theory. In this section we compare our results with other theories. We first examine the relationship between the present theory and the kinetic collision theory (KCT). In our model, the system is in equilibrium at $t<0$. Therefore, the reaction rate at $t=0$ is determined only by the equilibrium collision rate and the transmission coefficient α. The KCT expression for the initial rate constant $k^{\mathrm{KCT}}(0)$ is given by[20]

$$k^{\mathrm{KCT}}(0) = 2\pi R^2 \alpha \sqrt{\frac{2k_{\mathrm{B}}T}{\pi m}}. \tag{48}$$

Using the dimensionless variables and the reactivity parameter p, this equation is rewritten as

$$\varkappa^{\mathrm{KCT}}(0) = \frac{\alpha}{2} = \frac{p}{1+p}. \tag{49}$$

The reactivity parameter dependence of $\varkappa^{\mathrm{KCT}}(0)$ is exhibited in Fig. 4. We can recognize from Fig. 4 and Eqs. 41 and 49 that the short-time limiting value of the rate constant in the present theory is slightly larger than that in KCT. It should be noted, however, that Eq. 49 can be derived from the initial and boundary conditions in the present theory without referring to KCT. At $t=0$, $n_2(X, 0)$ must be $n_0/2$. Combining this relation with Eqs. 31,38,39, we obtain Eq. 49. This means that the present theory is consistent with KCT as far as the rate constant in the short-time limit is concerned. The small difference between Eqs. 41 and 49 is due to the approximation employed to solve the equation. We have already shown that the equation for the time evolution of $N(r, t)$ is non-local in time because of the approximation. See discussion below Eq. 25. The derivatives in the parentheses in the right-hand side of Eq. 25 are singular at $t=0$ and $r=R$, since $N(R, t)$ suddenly decreases at $t=0$ by the reaction. Thus, the effect of the approximation can appear even in the limit $t\rightarrow+0$. We later show that the small difference in $\varkappa(0)$ is not so important when we calculate the survival probability of target A.

Smoluchowski–Collins–Kimball Theory. In order to show the importance of the effects of inertia and non-Markovian friction, we next compare our result with the SCK theory[1,2] in which both of the two effects are neglected. In SCK theory, the simple diffusion equation is solved with the CK condition (Eq. 46). In Figs. 3 and 4, we depict the SCK results for two cases: one ($p=1.0$) coincides with the present results in the long-time limit; the other ($p=0.5$) coincides with Eq. 49 in the short-time limit. The latter has been recommended by Zhou and Szabo.[20] We think that a comparison between the present and SCK results for the same p is more reasonable because the long-time limits of the two theories are identical and the SCK theory is considered to be valid at long times.

From the figures, we can see that the decay of the SCK rate constant is much faster than that of the present result at short times. This indicates the importance of the inertia and non-Markovian effects in the short-time dynamics of diffusion-controlled reactions. In the inertialess limit as in the case of the SCK theory, the velocity distribution is always in equilibrium. When the inertia effect is taken into account, since it takes a finite duration to achieve a steady velocity distribution after the reaction begins, the variation of the reaction dynamics becomes slower. For this reason, the initial decay of $\varkappa(\tau)$ is faster in SCK theory than in the present treatment, even in the Markovian case. For the Markovian case, the present and SCK results for the same p are virtually identical at times longer than $\tau=4$. The velocity autocorrelation function for the Markovian case is nearly zero at $\tau=4$, and thus the inertia effect is expected to disappear. When the non-Markovian effect is taken into account in addition to the inertia effect, a slow variation in the velocity distribution is expected to be more pronounced; the decay of vacf is slower at $\rho^*=0.9428$ than at $\rho^*=0.7856$ when we compare them in the reduced time variable, $\tau=t\beta_\infty$. Therefore, the decay of $\varkappa(\tau)$ becomes more slow in the non-Markovian case. The difference in the rate constants at $\rho^*=0.9428$ and 0.7856 mentioned previously can be interpreted in this manner.

The effect of the boundary condition on the velocity distribution can be observed in the short-time limiting value of the rate constant $\varkappa(0)$. In Fig. 4, $\varkappa(0)$ in the SCK theory is compared with the present one. The SCK result is linear in p, and is always larger than the present one. This can be explained in the following way: In the present treatment, the time dependence of the density $N(X,\tau)$ at the reaction radius shows a discrete jump at $\tau=0$. The density at $r=R$ suddenly changes from n_0 to $(1+\alpha)n_0/2$ at $\tau=0$. On the other hand, the CK condition (Eq. 46) is expressed in terms of Fick's law, and the variation of $N(X,\tau)$ in the SCK theory is governed only by the diffusive (inertialess) flux, even at $\tau=0$. There are no discrete jumps in $N(X,\tau)$ around $\tau=0$, and $N(X,\tau\rightarrow+0)$ is always n_0. Therefore, $N(X,\tau\rightarrow+0)$ is smaller in the present treatment than in the SCK theory. Since $\varkappa(\tau)$ is given by $pN(X,\tau)/n_0$ in both the present and SCK theory, $\varkappa(0)$ is smaller in the present treatment than in the SCK theory. This result clearly indicates the importance of the boundary condition for the velocity distribution in a theoretical model for a diffusion-controlled reaction.

The SCK result for $p=0.5$ corresponds to Zhou and Szabo's[20] (ZS) extension of the SCK theory. They have pointed out that the SCK theory gives the exact rate constant at $t=0$ if k^{int} is given by $k^{\mathrm{KCT}}(0)$. For a collision-induced reaction with $\alpha=1$, the ZS theory shows a better agreement with the simulation than does the SCK theory for the absorbing boundary condition. There are the following two differences between the present treatment and the ZS theory: (1) The collision rate is assumed to be proportional to $N(X,\tau)$ in the

ZS theory, while the collision rate is proportional to $n_2(X,\tau)$ in the present treatment. (2) Since the simple diffusion equation is used in the ZS theory even in the short-time limit, the ZS rate constant decays rapidly at short times. From Figs. 2 and 3, we can see that the ZS rate constant is much smaller than the present result for $\tau>0$.

Dong–Andre Theory. Finally, we compare our result with the Dong–Andre (DA) theory.[6] In the DA theory, both the inertia and non-Markovian effects are taken into account using a generalized diffusion equation with a time-dependent diffusion constant derived by Mazo.[5] When the initial velocity distribution is Maxwellian, the time-dependent diffusion constant $D(t)$ is given by[5,6] (see Appendix)

$$D(t)=\frac{k_BT}{m}\psi(t)=\frac{1}{6}\frac{d}{dt}\langle[\boldsymbol{r}(t)-\boldsymbol{r}(0)]^2\rangle. \tag{50}$$

For the delta-function type friction kernel, this equations is identical to that derived by Morita.[21] Dong and Andre approximately solved the generalized diffusion equation with the CK condition, and obtained two expressions for the time-dependent rate constant: One is suitable for a short time and the other for a long time. In intermediate time regions, the larger of the two rate constants can be used as an approximation. As in the case of the SCK theory, we depict the DA results in Figs. 3 and 4 for the two cases, i.e., $p=1.0$ and 0.5. So far, we have no idea about how to judge which one is more suitable for a comparison with the present result. Although the long-time limiting value for $p=0.5$ is different from the present one, the short-time limit coincides to $\varkappa^{KCT}(0)$; the DA theory is expected to be valid at both short and long times.

Qualitatively, the DA rate constant shows similar tendencies to those found here: (1) The short-time limiting value of $\varkappa(\tau)$ is independent of the time-dependent friction kernel. (2) The decay of $\varkappa(\tau)$ is slower than the SCK result even for the Markovian case. (3) When the non-Markovian effect is present, the decay of $\varkappa(\tau)$ becomes slower at short times than that for the Markovian case. These resemblances in the results of two different approaches support the validity of each other. On the other hand, the short-time limiting value of the rate constant of the DA theory is larger than the present one and the same as that of the SCK theory by assumption[6] when we compare the results for the same p. We think that a further investigation is necessary to reveal the meaning of the difference between the DA and the present results.

Simulation

Model System. In order to test the validity of the present theory, we carried out a molecular dynamics simulation in a hard-sphere fluid. Molecular dynamics simulations for a diffusion-controlled reaction between hard-spheres in a hard-sphere fluid have been reported by Dong, Baros, and Andre[22] and Zhou and Szabo.[20] Their simulations clearly indicate the shortcomings of the simple Smoluchowski treatment at short times, and provide an important reference system in the study of reaction dynamics in solution. For the present purpose, on the other hand, we need a modification on their simulations. In the present theoretical treatment, we simplify the system by neglecting the potential effect to focus our attention exclusively on the dynamic effects of the inertia and the non-Markovian friction. As indicated by Zhou and Szabo,[20] however, the effect of the potential of mean force (PMF) cannot be neglected in their simulations.

The elimination of the effect of PMF from the model system is very important for a definite test of the present theory. The effect of PMF on the dynamic processes of diffusion-controlled reaction has not been thoroughly understood.[20] Therefore, if we compare our results with a simulation which includes the PMF effect, we cannot distinguish the shortcomings of the present theory from those of theoretical treatments of the PMF effect. For a better understanding of the PMF effect, we also need a simulation without the PMF effect as a reference system to separate the contribution of the PMF effect from those of other effects in determining the rate constant.

To eliminate the PMF effect we simulated an encounter reaction between a test particle and a moving hard-sphere. We assumed that there are no physical interactions between the test particle and the hard-spheres; since even the hard-core repulsive interaction was absent, the hard-spheres freely go through the test particle. The target is fixed in space. The reactants and the solvents are hard-spheres of the same mass and diameter. Therefore, the inter-diffusion coefficient between the target and the reactant is given by the self-diffusion coefficient of a one-component hard-sphere fluid. We assume that the target has the same diameter as the reactant, and is quenched when it overlaps with one of the reactants. This model system strictly corresponds to the model employed in the theoretical treatment for $p=1$

Method. The program for the molecular dynamics simulation is a modification of that given by Allen and Tildesley.[23] There are $N=500$ identical particles in a cubic cell for which the periodic boundary condition and the minimum image convention are applied. Initially, the N particles are put on the fcc lattice sites, and are given velocity using Gaussian random numbers. We carried out simulations at two densities, i.e., $\rho^*=0.7856$ and 0.9428. The system was equilibrated for more than 10^6 collisions before the run in order to obtain the survival probability at each density.

We next explain the simulation for the survival probability. At an arbitrary time after the system became equilibrated, we set $t=0$. We randomly chose N_B particles from the N moving particles and labeled them B. We simulated for $N_B=50$; we chose the N_B value to be as small as possible so as to obtain measurable time dependencies of the survival probabilities within reasonable uncertainties, since we needed to eliminate the effect of the interactions between the B molecules. We put 500 test particles on the fcc lattice sites in the same MD cell. We removed test particles which already overlapped with a B particle at $t=0$ from the system, and started the MD simulation with the remaining N_A test particles. For typical cases, $N_A=360$ and 330 at $\rho^*=0.7856$ and 0.9428, respectively. The positions of the N_A test particles were fixed during the MD simulation. We checked the overlaps between

the test and B particles at every MD steps, i.e., at every collision between any two of the N moving particles. We recorded the time t_j at which the j-th test particle overlapped with one of the B particles for the first time. The survival probability $S(t)$ of a test particle was calculated by

$$S(t) = \frac{1}{N_A} \sum_{j=1}^{N_A} \theta(t_j - t), \tag{51}$$

where $\theta(t)$ is the Heaviside step function. We averaged the survival probabilities for 1000 successive runs.

The velocity autocorrelation functions and the mean-square displacements used to calculate $\xi(t)$ and $\gamma(t)$ in GFPE and $D(t)$ in the DA theory were obtained from runs independent of those for the survival probabilities. The long-time diffusion coefficients D_∞ are 1.023- and 0.561-times as large as the Enskog values at $\rho^*=0.7856$ and 0.9428, respectively. The former agrees with the value by Easteal, Woolf, and Jolly[14] (EWJ) for 432 particles within the simulation uncertainty (3%). The latter lies between the EWJ values for 128 and 250 particles; EWJ did not make a simulation for 432 particles at $\rho^*=0.9428$.

Test of Theories. Now we compare the simulation results with the theoretical ones. The simulation results for $N_B=50$ at $\rho^*=0.7856$ and 0.9428 are shown in Figs. 5 and 6, respectively, with the theoretical results discussed in the previous sections. In Fig. 6, we omit the SCK predictions in order to avoid confusion. Theoretical survival probabilities were calculated from the time-dependent rate constant $k(t)$ by the following equation:

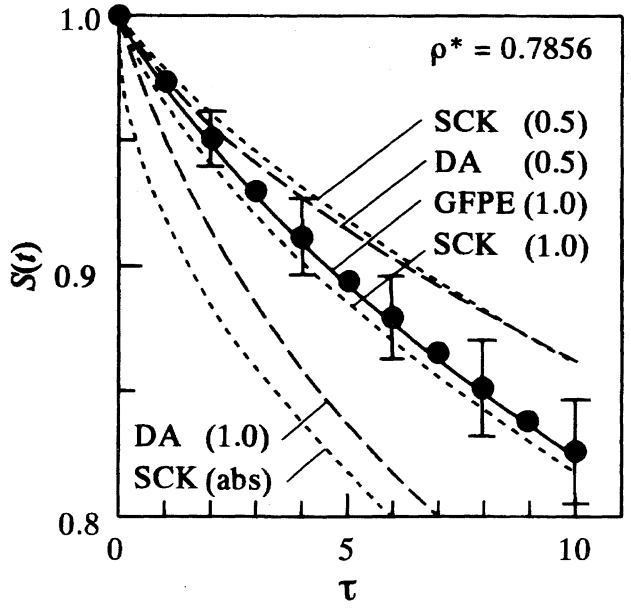

Fig. 5. Survival probabilities of a test particle in a hard-sphere fluid for $N_B/N=0.1$ at $\rho^*=0.7856$. Black circles indicate the average values of the simulation results. The heights of the error bars are two times as large as the standard deviations for 1000 runs. Lines and numbers have the same meanings as in Fig. 2. "abs" indicates the result for the absorbing boundary condition.

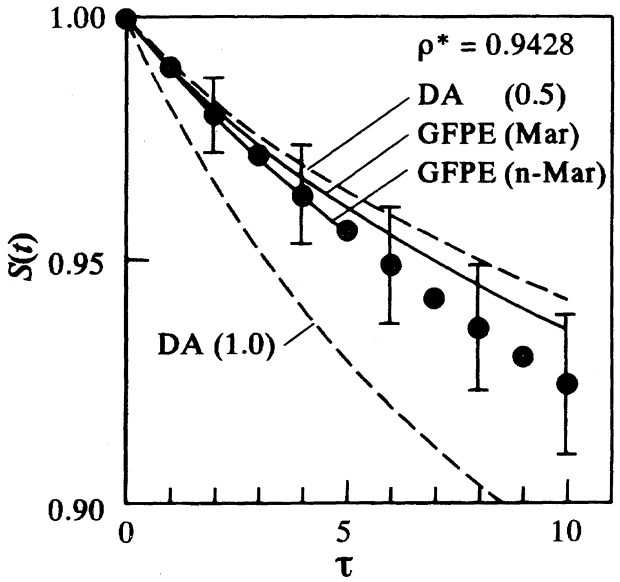

Fig. 6. Survival probabilities of a test particle in a hard-sphere fluid for $N_B/N=0.1$ at $\rho^*=0.9428$. Symbols, lines, numbers, and abbreviations have the same meanings as in Figs. 3 and 5. The results of this work are calculated for $p=1.0$.

$$S(t) = \exp\left[-\rho_B \int_0^t k(t')dt'\right], \tag{52}$$

where ρ_B is the concentration of the B particle, given by

$$\rho_B = \rho \frac{N_B}{N}, \tag{53}$$

and ρ is the number density of the N moving particles.

At $\rho^*=0.7856$, for which the non-Markovian effect is negligible, the present result agrees excellently with the simulation result. We should note that we used no adjustable parameters in the comparison between the present theory and the simulation; even the reactivity parameter was determined theoretically. Therefore, the validity of the present theory used to explain the inertia effect is obvious. From Eq. 52, we can see that the small error in the short-time limiting value of the rate constant mentioned in the previous section is not so important for the survival probability.

The SCK result for $p=1.0$ also reproduces the simulation results within the simulation uncertainty, although the SCK prediction slightly smaller than the average of the simulation result. This supports our opinion that the present and the SCK results should be compared for the same p value. The underestimation is due to the unphysically large short-time limiting value of the SCK rate constant. It should be noted, however, that the value of p (or k^{int}) which reproduces the simulation result, cannot be determined within the framework of the SCK theory. We need the help of the present treatment to explain the p value. The SCK result for $p=0.5$ cannot reproduce the simulation result in spite of the reasonable short-time limiting value of the rate constant.

In addition to the theoretical predictions discussed in the previous sections, we exhibit the prediction of the SCK theory for the absorbing boundary condition (so-called the sim-

ple Smoluchowski theory), because the absorbing boundary condition is usually considered to express the situation that the reaction occurs whenever A and B collide; this is the same situation as in the present simulation. It is obvious from Fig. 5 that the absorbing boundary condition is not suitable to describe the situation.

At $\rho^*=0.9428$, the present result for the non-Markovian case agrees with the simulation, though the prediction is calculated only for $\tau<5$. The agreement between the present result for the non-Markovian case and the simulation is obviously better than that for the Markovian case, although the two predictions are similar within the simulation uncertainty; the decay of $S(t)$ in the simulation is faster than the theoretical prediction for the Markovian case. This shows that the non-Markovian effect is non-negligible in the reaction dynamics in a dense fluid.

We do not consider the SCK results in Fig. 6 in order to avoid confusion. For $\tau<5$, the agreement between the SCK prediction for $p=1.0$ and the simulation result at $\rho^*=0.9428$ is better than at $\rho^*=0.7856$. However, the better agreement is a result of a cancellation of the large rate constant at $t=0$ and neglecting the non-Markovian effect.

At both of the densities studied, the DA theory cannot explain the simulation results. Although it is possible to use p as an adjustable parameter to seek the best-fit curve, we believe that it is not so meaningful, since there are no theoretical reasons to use the p values, except for $p=1.0$ and 0.5.

Summary

In this paper we have clarified the importance of the inertia and non-Markovian effects in determining the time-dependent rate constant of a diffusion-controlled reaction at short times, starting from the generalized Fokker–Planck equation. From a theoretical investigation we found the following tendencies: (1) The inertia effect slows down the decay of the rate constant. (2) The non-Markovian effect makes the decay slower. (3) The theoretical rate constant depends sensitively on the boundary condition for the velocity distribution. From the simulation we can conclude the following: (4) The present theory agrees excellently with the simulation for both the Markovian and the non-Markovian cases. (5) Although the SCK theory reasonably reproduces the simulation results for the Markovian case, we must be careful about the fact that the SCK theory overestimates the short-time limiting value of the rate constant. (6) The non-Markovian effect plays a non-negligible role in determining the reaction dynamics in dense fluids. We believe that our simple model describes the essential features of the short-time dynamics of diffusion-controlled reactions just as the SCK theory does concerning their long-time behavior.

Appendix: Derivation of Generalized Fokker–Planck Equation

We explain the outline of the derivation of GFPE (Eq. 8) based on the generalized Langevin equation (GLE) (Eq. 7) following the method by Mazo,[5] in order to clarify the assumptions included in the derivation. We explain only the one-dimensional case for simplicity.

The most important assumption made in the derivation is that the random force $F(t)$ is a second-order stationary Gaussian random variable. The other properties of $F(t)$ are that

$$\langle F(t)\rangle = 0, \tag{54}$$

$$\langle F(0)F(t)\rangle = mk_{\mathrm{B}}T\beta(t), \tag{55}$$

and

$$\langle v(0)F(t)\rangle = 0. \tag{56}$$

Equation 7 can be solved for the natural boundary as follows:

$$v(t) - v_0\chi(t) = \frac{1}{m}\int_0^t \chi(t-t')F(t')\mathrm{d}t' = y_1(t), \tag{57}$$

$$x(t) - x_0 - v_0\psi(t) = \frac{1}{m}\int_0^t \psi(t-t')F(t')\mathrm{d}t' = y_2(t), \tag{58}$$

where $v_0=v(0)$, $x_0=x(0)$, and $\chi(t)$ and $\psi(t)$ are given by Eqs. 12 and 11, respectively. From the above equations, we can see that $y_1(t)$ and $y_2(t)$ are Gaussian random variable, since they are linear functions of a Gaussian random variable $F(t)$. Therefore, the distribution function $P(\boldsymbol{y})$ for $\boldsymbol{y}=(y_1,y_2)$ is given by

$$P(\boldsymbol{y}) = \frac{1}{\pi\sqrt{|\det\boldsymbol{Q}|}}\exp(-\boldsymbol{y}^{\dagger}\boldsymbol{Q}^{-1}\boldsymbol{y}), \tag{59}$$

where $\boldsymbol{Q}$ is the covariance matrix. The components of $\boldsymbol{Q}$ are given by:

$$Q_{11} = \langle[v(t) - v_0\chi(t)]^2\rangle = \frac{k_{\mathrm{B}}T}{m}[1-\chi^2(t)], \tag{60}$$

$$\begin{aligned} Q_{12} = Q_{21} &= \langle[v(t) - v_0\chi(t)][x(t) - x_0 - v_0\psi(t)]\rangle \\ &= \frac{k_{\mathrm{B}}T}{m}\psi(t)[1-\chi(t)], \end{aligned} \tag{61}$$

$$Q_{22} = \langle[x(t)-x_0-v_0\psi(t)]^2\rangle = \frac{k_{\mathrm{B}}T}{m}\left(2\int_0^t \psi(t')\mathrm{d}t' - \psi^2(t)\right). \tag{62}$$

Q_{11}, Q_{12}, and Q_{22} are independent of v_0 and x_0. Equations 60, 61, and 62 can be derived using the fluctuation–dissipation relation, Eq. 55.[4]

We have obtained the distribution function $P(v, x)$, then we search for an equation satisfied by $P(v, x)$. The characteristic function $C(\lambda, \mu)$ is the Fourier transform of $P(v, x)$.

$$C(\lambda,\mu) = \langle\exp(i\lambda v + i\mu x)\rangle. \tag{63}$$

Since the probability distribution implicit in the angular brackets is Gaussian in this case, $C(\lambda, \mu)$ is also Gaussian. Then,

$$C(\lambda,\mu) = \exp\left[i\lambda v_0\chi + i\mu(x_0+v_0\psi) - \frac{1}{2}(\lambda^2Q_{11} + 2\lambda\mu Q_{12} + \mu^2Q_{22})\right]. \tag{64}$$

Differentiating this equation,

$$\frac{1}{C}\frac{\partial C}{\partial t} = i\lambda v_0\dot{\chi} + i\mu v_0\dot{\psi} - \frac{1}{2}(\lambda^2\dot{Q}_{11} + 2\lambda\mu\dot{Q}_{12} + \mu^2\dot{Q}_{22}) \tag{65}$$

and

$$\frac{1}{C}\frac{\partial C}{\partial \lambda} = iv_0\chi - \lambda Q_{11} - \mu Q_{12}. \tag{66}$$

Eliminating v_0 from Eqs. 65 and 66, and using Eqs. 60, 61, and 62, we obtain an equation for $C(\lambda, \mu)$,

$$\frac{\partial C}{\partial t}-\mu\frac{\partial C}{\partial \lambda}=\frac{\dot{\chi}}{\chi}\left(\lambda\frac{\partial C}{\partial \lambda}+\frac{k_BT}{m}\lambda^2 C\right)+\lambda\mu\left(\frac{\dot{\chi}}{\chi}\psi+1-\chi\right)C \quad (67)$$

We can obtain a one-dimensional generalized Fokker–Planck equation by an inverse Fourier transform of Eq. 67,

$$\frac{\partial P}{\partial t}+v\frac{\partial P}{\partial x}=-\frac{\dot{\chi}}{\chi}\frac{\partial}{\partial v}(vP)-\frac{\dot{\chi}}{\chi}\frac{k_BT}{m}\frac{\partial^2 P}{\partial v^2}-\left(\frac{\dot{\chi}}{\chi}\psi+1-\chi\right)\frac{k_BT}{m}\frac{\partial^2 P}{\partial x\partial v}. \quad (68)$$

Mazo[5] derived a generalized diffusion equation (GDE) from GLE by the same procedure as the derivation of GFPE. The distribution function in position $N(x, t)$ can be obtained from the distribution function in phase space by

$$N(x,t)=\int_{-\infty}^{\infty}P(v,x,t)\mathrm{d}v. \quad (69)$$

Therefore, the characteristic function for $N(x)$ is given by $C(\lambda=0, \mu)$, and

$$\frac{1}{C(0,\mu)}\frac{\partial C(0,\mu)}{\partial t}=i\mu v_0\chi-\frac{\mu^2}{2}\dot{Q}_{22}. \quad (70)$$

Taking inverse Fourier transformation, we obtain GDE,

$$\frac{\partial N(x,t)}{\partial t}=\frac{k_BT}{m}\psi(1-\chi)\frac{\partial^2 N(x,t)}{\partial x^2}-v_0\chi\frac{\partial N(x,t)}{\partial x}. \quad (71)$$

In the long-time limit, this equation reduces to the ordinary diffusion equation, since $\chi(\infty)=0$ and $k_BT\psi(\infty)/m=D_\infty$. By comparing it with the ordinary diffusion equation, Eq. 71 has an additional term which depends on the initial velocity v_0. A similar equation was derived for the Markovian case from OFPE by Morita.[21]

When the initial velocity distribution is Maxwellian, $C(0, \mu)$ should be averaged over the initial velocity; we thus obtain

$$\frac{1}{c(0,\mu)}\frac{\partial c(0,\mu)}{\partial t}=-\frac{\mu^2k_BT}{m}\psi, \quad (72)$$

where $c(0, \mu)$ is $C(0, \mu)$ averaged over the initial velocity. We then obtain GDE for a distribution function $n(x, t)$ with the Maxwellian initial velocity distribution by an inverse Fourier transformation of Eq. 72,

$$\frac{\partial N(x,t)}{\partial t}=\psi(t)\frac{k_BT}{m}\frac{\partial^2 N(x,t)}{\partial x^2}. \quad (73)$$

This is the starting equation of the DA theory.[6]

The authors are grateful to Professor S. A. Adelman and Professor T. Munakata for discussions concerning the validity of the generalized Fokker–Planck equation with singular coefficients. We also thank Mr. Y. Kubo for assistance in the computer simulation. This work was supported by Research Grant-in-Aid on Priority-Area-Research (Nos. 07228262 and 08218258) "Photoreaction Dynamics" from the Ministry of Education, Science and Culture.

References

1) M. von Smoluchowski, *Z. Phys. Chem.*, **92**, 129 (1917).
2) F. C. Collins and G. E. Kimball, *J. Colloid Sci.*, **4**, 425 (1949).
3) K. Ibuki and M. Nakahara, *J. Chem. Phys.*, **92**, 7323 (1990).
4) S. A. Adelman, *J. Chem. Phys.*, **64**, 124 (1976).
5) R. M. Mazo, in "Stochastic Process in Nonequilibrium Systems, " Vol. 84 of "Lecture Notes in Physics," ed by L. Garrido, P. Seglar, and P. J. Shepherd, Springer, Berlin (1978), p. 54.
6) W. Dong and J. C. Andre, *J. Chem. Phys.*, **101**, 299 (1994).
7) M. San Miguel and J. M. Sancho, *J. Stat. Phys.*, **22**, 605 (1980).
8) S. Harris, *J. Chem. Phys.*, **78**, 4698 (1983).
9) S. Harris, *J. Chem. Phys.*, **72**, 2659 (1980); **75**, 587, 3103 (1981); **77**, 934 (1982).
10) J.-P. Hansen and I. R. McDonald, "Theory of Simple Liquids," 2nd ed, Academic Press, London (1986), Chap. 7.
11) A. Rahman, *Phys. Rev. Sect. A*, **136**, 405 (1964).
12) G. D. Harp and B. J. Berne, *J. Chem. Phys.*, **49**, 1249 (1968).
13) B. J. Alder, D. M. Gass, and T. E. Wainwright, *J. Chem. Phys.*, **53**, 3813 (1970).
14) A. J. Easteal, L. A. Woolf, and D. L. Jolly, *Physica A (Amsterdam)*, **121**, 286 (1983).
15) P. Hänggi, H. Thomas, H. Grabert, and P. Talker, *J. Stat. Phys.*, **18**, 155 (1978).
16) This equation differs from the corresponding equation in Ref. 8 (Eq. 14) by the factor of $1/s$. In Ref. 8, the Laplace transform of the rate constant was defined as $\tilde{k}(s)\tilde{n}_0(s)=4\pi R^2|\tilde{j}_r(R,s)|$. This equation should be replaced by $\tilde{k}(s)n_0=-4\pi R^2\tilde{j}_r(R,s)$, and then we get Eq. 40.
17) H. Stehfest, *Commun. ACM*, **13**, 47 and 624 (1970).
18) A. Morita, *J. Chem. Phys.*, **96**, 3680 (1992).
19) R. A. Sack, *Physica (Amsterdam)*, **22**, 917 (1956).
20) H. X. Zhou and A. Szabo, *J. Chem. Phys.*, **95**, 5948 (1991).
21) A. Morita, *J. Math. Chem.*, **16**, 49 (1994).
22) W. Dong, F. Baros, and J. C. Andre, *J. Chem. Phys.*, **91**, 4643 (1989).
23) M. P. Allen and D. J. Tildesley, "Computer Simulations in Liquids," Oxford University, Oxford (1987).